

# Mass transfer rate measurement of short time liquid phase epitaxial growth using an electrochemical method

LAI-JUH CHEN, KAN-LIN HSUEH, CHI-CHAO WAN\*

*Department of Chemical Engineering, National Tsing Hua University, Hsin Chu, Taiwan 30043*

J. GONG

*Department of Electrical Engineering, National Tsing Hua University, Hsin Chu, Taiwan 30043*

Received 22 October 1990; revised 5 March 1991

Convective mass transfer phenomena become significant in sub-micrometre liquid phase epitaxial layer growth. An aqueous solution containing 0.01 M  $K_3Fe(CN)_6$  + 0.01 M  $K_4Fe(CN)_6$  + 1.0 M KOH in a Plexiglass vessel was used to simulate the fluid motion and mass transfer condition in liquid phase epitaxy. The mass transfer phenomena between the liquid phase epitaxial system and electrochemical system at mass transfer limiting condition are equivalent. This was theoretically and experimentally verified. The influence of growth conditions, such as growth time ( $40 \text{ ms} \leq t \leq 300 \text{ s}$ ), solution depth ( $0.625 \text{ cm} \leq H \leq 1.25 \text{ cm}$ ), and solution kinematic viscosity ( $0.0104 \text{ cm}^2 \text{ s}^{-1} \leq \nu \leq 0.0161 \text{ cm}^2 \text{ s}^{-1}$ ), on the growth rate of the epi-layer were simulated by the electrochemical method. The dependence of simulated epi-layer thickness,  $L'$ , on growth time,  $t$ , can be expressed as  $L' = \alpha t^\beta$ . When  $t \leq 0.1 \text{ s}$ , the convective mass transfer process predominates and  $\beta = 0.9 \pm 0.2$ . When  $t > 0.1 \text{ s}$ , the mass transfer rate is controlled by diffusion and  $\beta = 0.5 \pm 0.05$ .

## Notation

$A$	area of epi-layer or electrode ( $\text{cm}^2$ )	$L_d$	moving distance of slider (cm)
$A_d$	constant in Equations 4 and 5 ( $\text{cm}^3 \text{ A}^{-1} \text{ s}^{-1}$ )	$L_w$	well length in LPE and electrochemical system ( $L_w = 0.587 \text{ cm}$ ) (cm)
$A_c$	constant in Equations 12 and 13 ( $\text{cm}^3 \text{ A}^{-1} \text{ s}^{-1}$ )	$n$	number of charge transfer (equiv. $\text{mol}^{-1}$ )
$a$	constant in Equation 14 (-)	$Re$	Reynolds number in the LPE system ( $VL_w/\nu$ )
$C_b$	bulk concentration in the LPE system ( $\text{mol cm}^{-3}$ )	$Re'$	Reynolds number in the electrochemical system ( $VL_w/\nu$ )
$C'_b$	bulk concentration in the electrochemical system ( $\text{mol cm}^{-3}$ )	$Sc$	Schmidt number in the LPE system ( $\nu/D$ )
$C_i$	surface concentration in LPE system ( $\text{mol cm}^{-3}$ )	$Sc'$	Schmidt number in the electrochemical system ( $\nu/D'$ )
$C_s$	solid concentration of the epi-layer ( $\text{mol cm}^{-3}$ )	$Sh$	Sherwood number in the LPE system ( $k_m x/D$ )
$D$	diffusivity in the LPE system ( $\text{cm}^2 \text{ s}^{-1}$ )	$Sh'$	Sherwood number in the electrochemical system ( $k'_m x/D'$ )
$D'$	diffusivity in the electrochemical system ( $\text{cm}^2 \text{ s}^{-1}$ )	$t$	contact time of melt and substrate in LPE system or contact time of solution and electrode in electrochemical system (s)
$F$	Faraday number ( $\text{C mol}^{-1}$ )	$t_a$	approximate contact time (s)
$H$	solution depth (cm)	$V$	well moving velocity ( $\text{cm s}^{-1}$ )
$I$	electric current (A)	$W$	well width in LPE and electrochemical system ( $w = 0.813 \text{ cm}$ ) (cm)
$i$	electric current density ( $\text{A cm}^{-2}$ )	$x$	characteristic length (cm)
$k_m$	convective mass transfer coefficient in the LPE system ( $\text{cm s}^{-1}$ )	$y$	distance from the solid surface to the solution (cm)
$k'_m$	convective mass transfer coefficient in the electrochemical system ( $\text{cm s}^{-1}$ )	$\alpha$	constant in Equation 4
$L$	epi-layer thickness (cm)	$\beta$	constant in Equation 14
$L'$	simulated epi-layer thickness by electrochemical method (cm)	$\nu$	kinematic viscosity of solution ( $\text{cm}^2 \text{ s}^{-1}$ )

## 1. Introduction

The liquid phase epitaxial (LPE) technique originated by Nelson [17] is widely used to provide semiconduc-

tor and magnetic oxide films for optoelectronic, microwave and magnetic devices. The method of LPE is based on the idea that the solubility of a constituent in a liquid solvent decreases in response to decrease in

\* Author to whom all correspondence should be addressed.

temperature. Hence, by cooling an initially saturated solution, which is in contact with a single crystal seed, epitaxial deposition of the constituent on the seed surface can be obtained.

In liquid phase epitaxy, the growth rate of the epi-layer is controlled by the diffusion rate of crystallization material in the melt. The growth rates of epi-layers at various growth conditions were studied by Rode [1] and by Hsieh [2], etc. Their results can be applied to the layer growth where the melt is stationary. The epi-layer grows as long as the melt contacts the substrate. The active layer thickness of a InGaAsP double heterostructure layer should be sub-micrometric in order to achieve a minimum threshold current density [3, 4]. The required contact time to grow a sub-micrometric layer by the step cooling method is of the order of seconds [5, 6]. The layer thickness in a quantum well device is less than a second. During such a short contact time the melt is disturbed by the sliding movement of the graphite boat. The melt is not stationary. The growth rate within a short time is much higher than that predicted by the static model [1, 2]. The high growth rate can be attributed to two possible causes. One is that the kinetics of crystallization predominates at the instance of crystallization [7]; the other is that the growth rate is governed by the convective mass transfer mechanism. A dyed aqueous solution was used to simulate the melt motion during short contact times [8]. The motion of the melt causes the convective mass transfer and the growth rate is enhanced. At present, the convective mass transfer phenomena under such conditions have not been well studied.

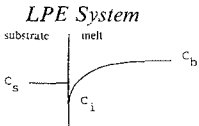
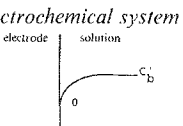
The aim of the present study is to evaluate the layer

growth rate with short contact times. An electrochemical method was adopted to measure the mass transfer rate under short contact time conditions and an aqueous electrolyte was used to simulate the melt movement. By controlling the electrode potential at the mass transfer limiting condition, the convective mass transfer rate of the electrochemical active species was obtained by measuring the current flow through the electrode. This method has been used to measure the convective mass transfer rates in many fluid flow systems [9–13]. By using this method, the effect of crystallization kinetics is eliminated. A theoretical comparison of diffusive and convective mass transfer behaviour between the liquid phase epitaxial system and the electrochemical system is first discussed.

## 2. Theoretical aspects

The concentration profiles of the LPE system and of the electrochemical system are schematically presented in Table 1. In the LPE system, the difference in concentration between the bulk ( $C_b$ ) and the epitaxial layer/melt interface ( $C_i$ ) causes the diffusion of the solute. At the epitaxial layer/melt interface thermodynamic equilibrium is established between the interfacial concentration at the melt side ( $C_i$ ) and at the solid side ( $C_s$ ). In the electrochemical system the electrochemical active species diffuses from the bulk with a concentration of  $C_b$  to the electrode surface. The electrode potential is controlled at the mass transfer limiting condition. Under the mass transfer limiting condition the concentration of electrochemical active species at the electrode surface is approximately zero.

Table 1. Schematic comparison between the LPE system and the electrochemical system

	LPE System 	Electrochemical system 
Governing equation	$\frac{\partial C}{\partial t} = D \frac{\partial^2 C}{\partial y^2}$	$\frac{\partial C'}{\partial t} = D' \frac{\partial^2 C'}{\partial y^2}$
Initial and boundary conditions	$C(0, y) = C_b$ $C(t, 0) = C_i$ $C(t, \infty) = C_b$	$C'(0, y) = C_b$ $C'(t, 0) = 0$ $C'(t, \infty) = C_b$
Concentration profile	$C = C_b - (C_b - C_i) \operatorname{erf} c \left( \frac{y}{2\sqrt{Dt}} \right)$	$C' = C_b \operatorname{erf} \left( \frac{y}{2\sqrt{D't}} \right)$
Material balance at interface	$D \frac{\partial C}{\partial y} \Big _{y=0} + (C_i - C_s) \frac{dL}{dt} = 0$	$i = nFD' \frac{\partial C'}{\partial y} \Big _{y=0}$
Growth rate	$\frac{dL}{dt} = \left( \frac{D}{\pi} \right)^{0.5} \left( \frac{C_b - C_i}{C_s - C_i} \right) t^{-1/2}$	$i = nF \left( \frac{D'}{\pi} \right)^{0.5} C_b t^{-1/2}$
<i>Physical properties</i>	<i>LPE system</i>	<i>Electrochemical system</i>
viscosity, $\mu$ (centipoise)	0.754 at 700°C*	1.005 at 20°C
density, $\rho$ (g cm <sup>-3</sup> )	5.61 at 700°C*	0.998 at 20°C
kinematic viscosity, $\nu = \mu/\rho$ (cm <sup>2</sup> s <sup>-1</sup> )	0.00134	0.01007
diffusivity of active species, $D$ (cm <sup>2</sup> s <sup>-1</sup> )	$1 \times 10^{-6} - 1 \times 10^{-5} \dagger$	$1.2 \times 10^{-5}$

\* Estimated by 700°C Ga melt in Ga rich growth solution (Ga wt % > 95%).

† Varied by different active species and growth temperature.

The material balances and initial and boundary conditions of both systems are listed in Table 1. The governing equations for both systems were obtained by assuming that the solution is stationary and only diffusion in the  $y$ -direction is considered. The flow of solution caused by the movement of the epitaxial layer/melt interface is negligible. Based on the governing equations and corresponding initial and boundary conditions, the concentration profiles for both systems can be solved and are also listed in Table 1. The typical physical properties of the LPE and electrochemical systems are also listed in Table 1. In the LPE system the physical properties are estimated for the 700°C Ga melt in a Ga rich growth solution (Ga wt % > 95%). At the epitaxial layer/melt interface the epi-layer thickness ( $L$ ) increases with a rate  $dL/dt$ . As the layer grows the volume of melt (with concentration of  $C_i$ ) is replaced by the solid (with concentration of  $C_s$ ) at a rate of  $A dL/dt$ . Here  $A$  is the area of the epi-layer. The net amount of material change  $(C_i - C_s) A (dL/dt)$ , is balanced by the diffusion rate at the interface  $(-DA(\partial C/\partial y)|_{y=0})$ . Substituting the concentration profile into the material balance equation at the interface the growth rate of the epi-layer  $dL/dt$  is:

$$\frac{dL}{dt} = \left(\frac{D}{\pi}\right)^{1/2} \left(\frac{C_b - C_i}{C_s - C_i}\right) t^{-1/2} \quad (1)$$

For the electrochemical system, a reversible electrochemical reaction, such as  $\text{Fe}(\text{CN})_6^{-3} + e^- \rightarrow \text{Fe}(\text{CN})_6^{-4}$ , takes place at the electrode surface where solution contacts the electrode. Therefore, the current is equal to the diffusion rate of  $\text{Fe}(\text{CN})_6^{-3}$  ions from the bulk to the electrode surface. Substituting the concentration profile into the material balance equation at the interface, the relation between the current density and contact time,  $t$ , can be expressed as:

$$i = nF \left(\frac{D}{\pi}\right)^{1/2} C_b' t^{-1/2} \quad (2)$$

Equation 1 divided by Equation 2, gives:

$$\frac{dL/dt}{i} = \frac{1}{nF} \left(\frac{D}{D'}\right)^{1/2} \left(\frac{C_b - C_i}{C_b'(C_s - C_i)}\right) \quad (3)$$

At a given growth temperature  $C_i$  and  $C_s$  are constants. Therefore, Equation 3 can be expressed as:

$$dL/dt = A_d i = \frac{1}{2} \alpha t^{-1/2} \quad (4)$$

where

$$A_d = \frac{1}{nF} \left(\frac{D}{D'}\right)^{1/2} \left(\frac{C_b - C_i}{C_b'(C_s - C_i)}\right) \quad (5)$$

From Equations 1 and 2 the terms  $dL/dt$  and  $A_d i$  are both proportional to  $t^{-1/2}$  as shown in Equation 4. Integration of Equation 4 gives:

$$L = A_d \int_0^t i dt = \alpha t^{1/2} \quad (6)$$

A plot of  $\ln L$  against  $\ln t$  or  $\ln \int_0^t i dt$  against  $\ln t$  yields a straight line with a slope of 0.5. Equation 6 indicates that for a stationary solution, the thickness

of an epi-layer after contact time,  $t$ , can be calculated from the current density,  $i$ , of an electrochemical system. The values of  $A_d$  or  $\alpha$  are constant only on the condition that the epi-layer grows at a constant temperature (step cooling condition). If the temperature is varied during the epi-layer growth the value of  $A_d$  is a function of time and ' $A_d$ ' should be included inside the integral of Equation 6.

Since the mass transfer behaviour with a short contact time is very complicated, an approximate analysis is given here. With a short contact time, the fluid is in motion and the epi-layer growth rate is controlled by the convective mass transfer rate of the deposited species in the melt. The material balance equation at interface can be rewritten as:

$$(C_i - C_s) \frac{dL}{dt} = k_m (C_b - C_i) \quad (7)$$

where  $k_m$  is the convective mass transfer coefficient. Under a similar situation as the LPE system the current density in the mass transfer limiting condition of the electrochemical system is controlled by the convective mass transfer rate of the reacting species in the solution:

$$i = nF k_m' C_b' \quad (8)$$

where  $k_m'$  is the convective mass transfer coefficient. In dimensional analysis, the convective mass transfer coefficient,  $k_m$  is usually correlated as a dimensionless variable, the Sherwood number,  $Sh$ . The Sherwood number can be experimentally correlated as a function of Reynolds number,  $Re$ , and Schmidt number,  $Sc$ .

$$Sh = \frac{k_m x}{D} = f_1(Re) f_2(Sc) \quad (9)$$

With similar geometry and fluid motion the Sherwood number for the electrochemical system can also be correlated as

$$Sh' = \frac{k_m' x}{D'} = f_1(Re') f_2(Sc') \quad (10)$$

As long as the electrochemical measurement is carried out at the same Reynolds number and Schmidt number as in the LPE system the relation between  $k_m$  and  $k_m'$  is

$$k_m = k_m' \frac{D}{D'} \quad (11)$$

Combining Equations 7, 8 and 11 the epi-layer thickness at a given contact time is:

$$\begin{aligned} L &= \frac{D}{nFD'} \left(\frac{C_b - C_i}{(C_i - C_s)C_b'}\right) \int_0^t i dt \\ &= A_c \int_0^t i dt \end{aligned} \quad (12)$$

where,

$$A_c = (D/nFD')[(C_b - C_i)/((C_i - C_s)C_b')] \quad (13)$$

At a given temperature and solution  $A_c$  is a constant. The layer thickness is proportional to the term  $\int_0^t i dt$  with a short contact time.

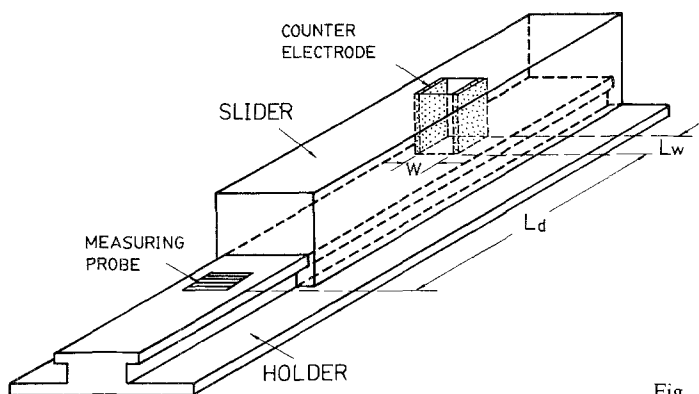


Fig. 1. Electrochemical cell for the mass transfer rate measurement.

### 3. Experimental details

The mass transfer rate measurements were carried out in a Plexiglass cell. The dimensions of this cell were similar to the dimensions of the graphite boat in the LPE system (Fig. 1). The cell contained a slider, a holder and a well on the slider. The well was filled with an aqueous electrolyte containing 0.01 M  $K_3Fe(CN)_6$ , 0.01M  $K_4Fe(CN)_6$ , and 1.0M KOH (all MERCK analytical grade). Two nickel plates with a total exposed area of  $1\text{ cm}^2$  were used as the counter electrode as well as the reference electrode. A measuring probe was flush mounted on the holder. The probe contained a sectioned nickel electrode and was made of five nickel plates. These were bonded and insulated by epoxy between the plates. The dimension of the plate exposed to the electrolyte was 0.587 cm wide and 0.813 cm in length. Since the insulation layer is less than 0.01 cm thick, the inactive area is negligible, and the sectioned electrode can conceptually simulate the LPE system.

The slider was pushed by a stepping motor (Sanyo Denki Co., Ltd, 103-845-2), which was driven by a PM-driver (Sanyo Denki, Co., Ltd, PMM-UA-4302). The potentials of the sectioned electrode were controlled by a homemade multi-potentiostat. The multi-potentiostat controlled the sectioned electrode potential in the mass transfer limiting region and measured the current at each electrode individually. The electrical circuit was similar to the bi-potentiostat [14]. Control of the slider movement, electrode potentials, and current measurement was carried out by a personal computer with a multi-channel data acquisition system (Advantech Co., Ltd, AD500A).

The region of potential in which mass transfer occurs at limiting condition was first measured. The measuring probe was placed in a cell where the electrolyte flowed between two parallel plates. The gap between the plates was 0.635 cm. One plate was made of nickel and served as the reference as well as the counter electrode. The measuring probe was flush mounted on the other plate and was placed 28.2 cm from the flow entrance. The other plate was made of Plexiglass. The electrode potentials were scanned from 0 to 1.5 V at different flow rates ( $3.08 \sim 16.82\text{ cm s}^{-1}$ ). The potential region for the mass transfer limiting

condition was observed to be from 0.2 to 1.2 V. The potential of each electrode was kept at 0.8 V in the mass transfer rate measurements.

Before the mass transfer measurement the electrode was polished, degreased, and rinsed. The probe was flush mounted on the holder. The gap between the slider and holder was filled with silicone to avoid leakage of electrolyte. The electrode potentials were pre-set at 0.8 V. The slider was driven by a stepping motor at a constant speed. When the wall was located right on top of the probe the slider was stopped. After a given time the slider was pushed away. The current flowing at each electrode was recorded as a function of time.

### 4. Results

The mass transfer rate measurement with a stationary electrolyte is presented in Fig. 2 where value of  $\int_0^t I dt$  is plotted against  $t$  on a  $\ln$ - $\ln$  scale. A straight line with a slope of 0.5 was obtained. The experimental result is consistent with Equation 6. For the step cooling method in the LPE system the layer thickness is proportional to  $t^{1/2}$  and was experimentally verified [2]. Figure 2 suggests that in a stagnant solution, the time dependencies of mass transfer rate in both the LPE system and electrochemical system are equivalent.

During the simulation of short time LPE the well

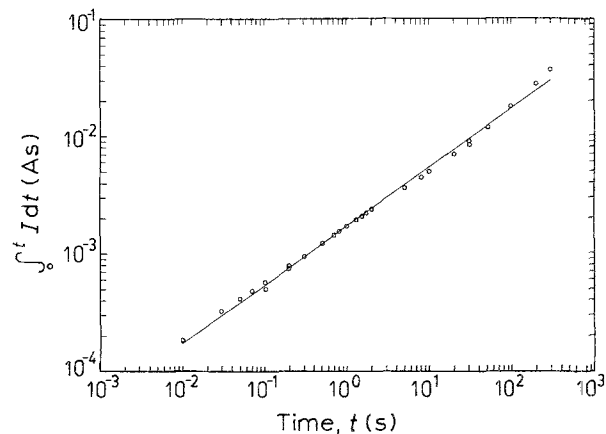


Fig. 2. The mass transfer rate measurement in a stationary solution. A plot of  $\ln \int_0^t I dt$  against  $\ln t$ .  $V = 0\text{ cm s}^{-1}$ ,  $H = 1.25\text{ cm}$ . (O) experimental plot, (—) theoretical line (slope = 0.5).

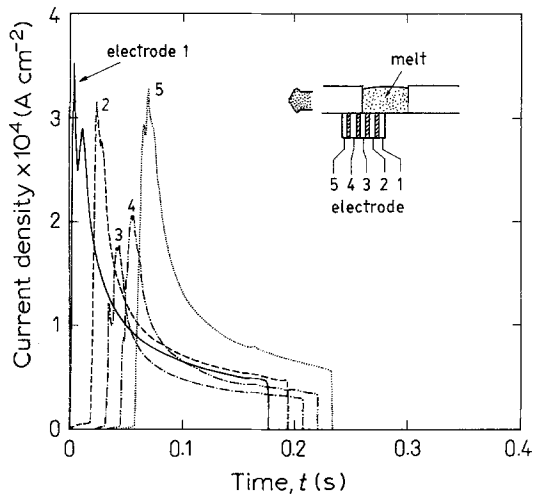


Fig. 3. Instantaneous current densities under a short contact time.  $H = 1.25$  cm,  $t = 0.177$  s,  $L_d = 1.125$  cm.  $V = 31.25$  cm s $^{-1}$ .

filled with electrolyte was moved toward the probe. When the well reached the position right on the top of the probe the slider stopped for a certain time; then the slider was moved away. The current densities of each electrode were recorded as a function of time and these are given in Fig. 3. The current density rose rapidly as the electrode made contact with the electrolyte and then decreased gradually. The current densities peaked at different times due to each electrode making contact with the electrolyte at different times. However, the actual contact times,  $t$ , for each electrode were the same.

A plot of  $\ln(\int_0^t I dt)$  against  $\ln t$  is given in Fig. 4 and two linear regions are observed. When the contact time  $t$  is longer than 0.1 s the time dependence of  $\ln \int_0^t I dt$  with a slope of 0.53 is obtained. A diffusion mechanism controls the mass transfer rate in this region. When the contact time is shorter than 0.1 s a slope of 0.83 is observed. This indicates that a convective mass transfer mechanism predominates. The quantity  $\int_0^t I dt$  can be regarded as the epi-layer thickness in the LPE system from Equation 6. From the hydrodynamic point of view there are several factors that may effect the growth rate of the epi-layer. The influences of these factors on the growth rate or mass

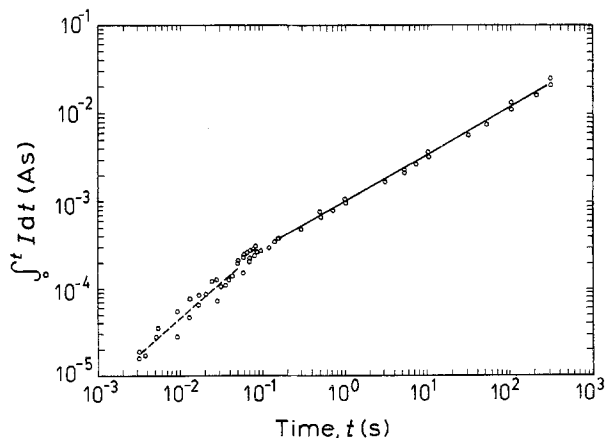


Fig. 4. A plot of  $\ln(\int_0^t I dt)$  against  $\ln t$ ,  $H = 1.25$  cm,  $L_d = 1.125$  cm,  $V = 31.25$  cm s $^{-1}$ . (---)  $\ln(\int_0^t I dt) = 0.8281 \ln(t) - 6.1602$ ; (-)  $\ln(\int_0^t I dt) = 0.5343 \ln(t) - 6.8759$ .

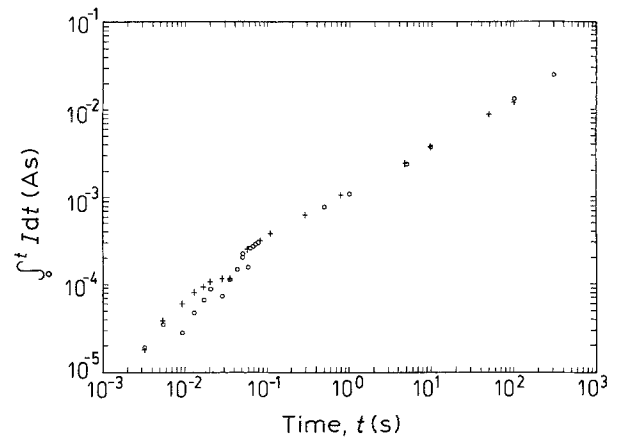


Fig. 5. Comparison of  $\ln(\int_0^t I dt)$  against  $\ln t$  curves at two different moving distances,  $L_d$ : (O) 1.125 and (+) 6.75 cm.  $H = 1.25$  cm,  $V = 31.25$  cm s $^{-1}$ .

transfer rate in the LPE system were simulated by the electrochemical system.

## 5. Discussion

When the slider starts moving, the hydrodynamic boundary layer at the interface of electrolyte and holder surface begins to develop. At a constant moving speed the thickness of the boundary layer is dependent on the movement distance of the slider,  $L_d$  (Fig. 1). A comparison of the mass transfer rate at two different values of  $L_d$  (1.125 cm and 6.75 cm) is given in Fig. 5. For a long reaction time, the motion of the electrolyte eventually dies down. As shown in Fig. 5, in the region of long contact time ( $t > 0.1$  s), the mass transfer rate is controlled by diffusion and the distance  $L_d$  is not important. The lines of  $\ln \int_0^t I dt$  against  $\ln t$  for two different values of  $L_d$  in the region of long contact time almost coincide with each other. The slopes of these lines are 0.53 and 0.51 for  $L_d = 1.125$  cm and 6.75 cm, respectively. In the region of short contact time ( $t < 0.1$  s) there is a difference in the mass transfer rate between two distances.

In a real LPE growth system the melt height is an important factor concerning the melt carry-over problem [15, 16]. The mass transfer rates in the electro-

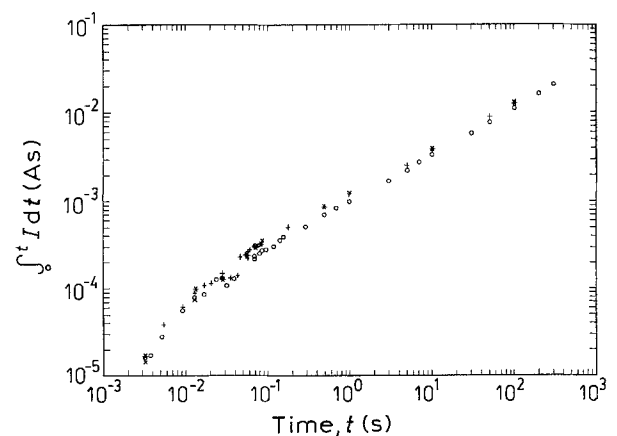


Fig. 6. Plot of  $\ln(\int_0^t I dt)$  against  $\ln t$  at different solution height  $V = 31.25$  cm s $^{-1}$ ,  $L_d = 1.125$  cm. H: (O) 1.250, (+) 0.625, (\*) 0.875 and (x) 1.125 cm.

chemical system at different solution depth,  $H$ , are compared in Fig. 6. There is no significant change of mass transfer rate as the solution depth changes in the range from 0.625 cm to 1.25 cm. This suggests that the mass transfer boundary layer thickness is much smaller than the solution depth. For a short contact time the mass transfer process takes place within a thin layer at the vicinity of the electrolyte/electrode interface. The solution depth is not affected. In the long contact time region the electrolyte is stationary and the mass transfer boundary layer does not reach to the top of the electrolyte.

In certain cases of LPE growth a cap covers the well to avoid the evaporation of crystallization species. In the well without a cap there is a free surface motion on the top of melt. In the well with a cap the cap/melt interface provides an extra solid boundary. The influence of the cap on the mass transfer rate was also studied. Fig. 7 compares the mass transfer rates of an electrochemical system between the electrolyte well covered with a cap and without a cap. It shows that the cap slightly enhances the mass transfer rate for short contact time but does not affect it for long contact time.

The dependence of mass transfer rate on the electrolyte viscosity was also examined. The increasing of electrolyte viscosity was obtained by adding NaCl to the electrolyte. The kinematic viscosities of the electrolyte without NaCl, added 3 M NaCl, and 6 M NaCl, are  $1.04 \times 10^{-2}$ ,  $1.28 \times 10^{-2}$ , and  $1.61 \times 10^{-2} \text{ cm}^2 \text{ s}^{-1}$ , respectively. The influence of kinematic viscosity on the short time mass transfer region is not clear (Fig. 8). Higher kinematic viscosity causes lower diffusivity. The mass transfer rates in the long contact time region are decreased due to the increases in kinematic viscosity. In real LPE systems the kinematic viscosity is about  $0.001 \text{ cm}^2 \text{ s}^{-1}$ . This is primarily due to a higher density of the melt than to the density of the aqueous electrolyte. Due to experimental limitations an electrolyte with high density was not found and only a narrow kinematic viscosity region was studied here.

In general, the dependence of the simulated epi-

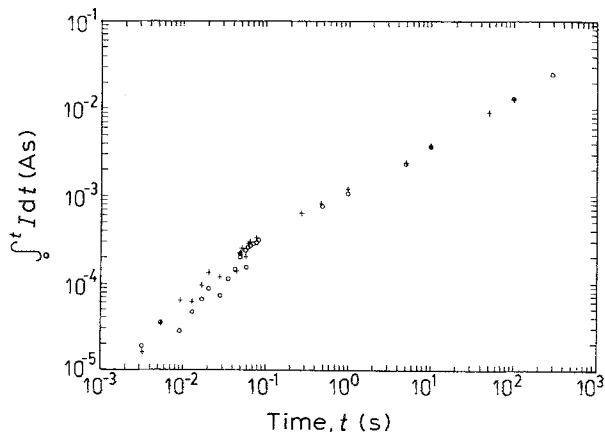


Fig. 7. Comparison of  $\ln \int_0^t I dt$  against  $\ln t$  curves. One with a cap on top of the electrolyte (O,  $H = 1.25 \text{ cm}$ ) and the other one without a cap (+,  $H = 0.625 \text{ cm}$ ).

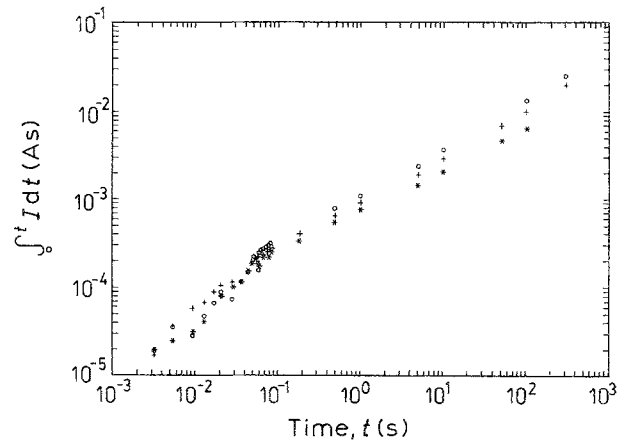


Fig. 8. Dependence of  $\int_0^t I dt$  against  $t$  on kinematic viscosity,  $\nu$ : (O)  $1.04 \times 10^{-2}$ , (+)  $1.28 \times 10^{-2}$  and (\*)  $1.61 \times 10^{-2} \text{ cm}^2 \text{ s}^{-1}$ .

layer thickness ( $L'$ ) on  $t$  can be divided into two parts ( $t < 0.1 \text{ s}$  and  $t \geq 0.1 \text{ s}$ ) and can be expressed as

$$\ln(L') = \alpha + \beta \ln t \quad (14)$$

or

$$L' = \alpha t^\beta \quad (15)$$

The values of  $\beta$  in the regions  $t < 0.1 \text{ s}$  and  $t \geq 0.1 \text{ s}$  at different situations are  $0.9 \pm 0.2$  and  $0.5 \pm 0.05$ , respectively.

## 6. Conclusion

An electrochemical method was proposed to simulate the convective mass transfer phenomena for the epi-layer growth by a step cooling LPE technique. The mass transfer behaviour of the electrochemical system was verified both theoretically and experimentally to be similar to the LPE system. In general, the mass transfer process of the electrochemical system within the time domain (40 ms  $\sim$  300 s) can be divided into two parts. When  $t < 0.1 \text{ s}$  the convective mass transfer process predominates. When  $t > 0.1 \text{ s}$  the electrolyte is almost stationary and a diffusional mass transfer behaviour is observed. The simulated epi-layer thickness ( $L'$ ) can be expressed as a function of contact time  $t$ :

$$L' = \alpha t^\beta \quad (16)$$

The values of  $\beta$  are  $0.9 \pm 0.2$  and  $0.5 \pm 0.05$  for  $t < 0.1 \text{ s}$  and for  $t > 0.1 \text{ s}$  respectively. Several factors in real LPE operation were also studied by the electrochemical system. A long slider moving distance or addition of a cap on the well slightly enhances the value of  $L$  for short contact time but there is no effect for long contact times. The melt height within the present studied region ( $0.625 \text{ cm} \leq H \leq 1.250 \text{ cm}$ ) also has no effect on the growth rate of the epi-layer.

## Acknowledgement

This work was supported by a contract (NSC77-0608-E007-03) to the National Tsing Hua University from the National Science Council.

**References**

- [1] D. L. Rode, *J. Crystal Growth* **20** (1973) 13.  
[2] J. J. Hsieh, *ibid.* **27** (1974) 49.  
[3] M. Yano, H. Nishi and M. Takusagawa, *IEEE J. Quantum Electronics* **QE-15** (1979) 571.  
[4] D. Botez, *ibid.* **QE-17** (1981) 178.  
[5] E. A. Rezek, B. A. Vojak, R. Chin, N. Holonyak Jr. and E. A. Sammann, *J. Electronic Materials* **10** (1981) 255.  
[6] C. L. Reynolds Jr., M. C. Tamargo, P. J. Anthony and J. L. Zilko, *J. Crystal Growth* **57** (1982) 109.  
[7] T. Henry and T. Minden, *ibid.* **6** (1970) 228.  
[8] S. Y. Leung and N. E. Schumaker, *ibid.* **60** (1982) 421.  
[9] M. Eisenberg, C. W. Tobias and C. R. Wilke, *J. Electrochem. Soc.* **103** (1954) 413.  
[10] D-T. Chin and M. Litt, *ibid.* **119** (1972) 1338.  
[11] D-T. Chin and C. H. Tsang, *ibid.* **125** (1978) 1461.  
[12] K-L. Hsueh and D-T. Chin, *ibid.* **133** (1986) 75 and **133** (1986) 1845.  
[13] D-T. Chin and K-L. Hsueh, *Electrochim. Acta* **31** (1986) 561.  
[14] A. Bard and L. R. Faulkner, 'Electrochemical Methods – Fundamentals and Applications', J. Wiley & Sons, New York, (1980) p. 567.  
[15] R. B. Wilson, P. Besomi and R. J. Nelson, *J. Electrochem. Soc.* **132** (1985) 172.  
[16] P. Besomi, R. B. Wilson and R. J. Nelson, *ibid.* **132** (1985) 176.  
[17] H. Nelson, *RCA Rev.* **24** (1963) 603.